coatings

MDPI

Article

Preparation of Weather-Resistant Nano-Coating Materials and Its Application in the Protection of Ancient Building Paintings

Jinglong Yang [1], Jiahe Zeng [2,3], Weihong Zhang [4], Siping Huang [4], Haoming Yang [5], Tao Wang [1], Xinjie Yu [6] and Jing Cao [2,3,*]

[1] Cultural Relics Protection Center of Xianyang City, Xianyang 712000, China; yjl313221@163.com (J.Y.); wtlybnhal@sina.com (T.W.)
[2] Key Laboratory of Archaeological Exploration and Cultural Heritage Conservation Technology, Northwestern Polytechnical University, Xi'an 710072, China; zjh3421241093@mail.nwpu.edu.cn
[3] NPU Institute of Culture and Heritage (NICN), Northwestern Polytechnical University, Xi'an 710072, China
[4] School of Chemistry and Chemical Engineering, Xianyang Normal University, Xianyang 712000, China; zwh10430@sina.com (W.Z.); huangsiping1971@163.com (S.H.)
[5] Department of History and Archaeology of Science and Technology, School of Humanities and Social Sciences, University of Science and Technology of China, Hefei 230026, China; twpqeqr0226@163.com
[6] School of Economics and Management, Nanchang Vocational University, Nanchang 330500, China; 15292779167@163.com
* Correspondence: jingcao@snnu.edu.cn

Abstract

In this study, to address the problems of fading and cracking of ancient architectural paintings caused by environmental aging, a weather-resistant nano-coating material was prepared using self-made nano-zinc oxide as the UV agent and water-based fluorocarbon coating as the binder. Taking slides and painted wooden boards as the coating objects, respectively, the transparency, ultraviolet absorption capacity, and weather resistance of the coating were detected by ultraviolet-visible spectrophotometer and ultraviolet light weather resistance test chamber. The test results show that the coating material not only has high transparency but also has obvious color retention and crack resistance effects on the painted layer. At present, this coating material has been successfully applied in the experimental research on the protection of painted cultural relics in Xianyang Museum and Zhaoren Temple in Changwu.

Keywords: nano-zinc oxide; water-based fluorocarbon coating; weather-resistance; color painting protection

Academic Editors: Maurizio Licchelli and Kirill A. Emelyanenko

Received: 27 June 2025
Revised: 21 September 2025
Accepted: 24 September 2025
Published: 4 October 2025

Citation: Yang, J.; Zeng, J.; Zhang, W.; Huang, S.; Yang, H.; Wang, T.; Yu, X.; Cao, J. Preparation of Weather-Resistant Nano-Coating Materials and Its Application in the Protection of Ancient Building Paintings. *Coatings* **2025**, *15*, 1161. https://doi.org/10.3390/coatings15101161

1. Introduction

China boasts a long history and rich cultural heritage, among which ancient architectural polychromy is one of the most representative art forms. These polychromies not only possess immense artistic value but also contain abundant historical and cultural information. However, over time, many ancient building polychromies have suffered from issues such as fading and cracking, severely impacting their artistic and historical value. Therefore, how to effectively protect these precious polychromic cultural heritages has become an important topic in the field of cultural relic protection [1–3].

In recent years, scholars both domestically and internationally have conducted extensive research on the conservation of ancient building paintings. Studies show that ultraviolet light from sunlight is one of the primary causes of fading and cracking in these paintings. Ultraviolet light can cause photochemical reactions in the organic components

of paint pigments, leading to color loss. Additionally, ultraviolet light can lead to thermal expansion coefficient differences between the painting layer and the ground layer, causing cracking [1,4–6]. To address this issue, researchers have tried various protective methods, including using silicone materials [2], nano-titanium dioxide [3], and nano-zinc oxide [7] as UV shields, as well as employing water-based fluorocarbon coating [8] as a binder. These materials can improve the weather resistance of paintings to some extent, but they still have certain limitations.

For example, although silicone materials have good weather resistance and breathability, their adhesion to the painted layer is poor [9–11]; while nano-titanium dioxide has strong UV shielding capabilities, it is less transparent in the visible light range [12]; and nano-zinc oxide, though effective in UV shielding and antibacterial properties, has poor dispersibility and tends to agglomerate [13]. Moreover, water-based fluorocarbon coatings used in some studies, although excellent in weather resistance and transparency, are costly and require complex application techniques in practical use [14].

To solve the problem of fading and cracking of ancient building paintings due to environmental aging, this study employs nano-zinc oxide with strong UV shielding and antibacterial properties, along with water-based fluorocarbon coatings that have excellent adhesion, permeability, and weather resistance and remain colorless and transparent after curing. These materials are mixed in specific proportions to create a transparent, anti-UV, and crack-resistant coating. The coating was applied to glass slides and painted wooden boards, and systematic research was conducted in the laboratory to evaluate its UV protection and crack resistance, achieving favorable experimental results. Additionally, a distinctive feature of this study is the high transparency and superior dispersibility of the self-made nano-zinc oxide, which not only enhances the coating material's performance in UV protection, color retention, and crack resistance but also offers high economic efficiency and ease of application. Currently, this product has been successfully implemented in the conservation and restoration of cultural relics.

2. Test Section

2.1. Test Materials

Zinc nitrate hexahydrate, analytical reagent grade, Tianjin Kemiao Chemical Reagents Co., Ltd. (Tianjin, China); anhydrous sodium carbonate, analytical reagent grade, Tianjin Hongyan Reagent Factory (Tianjin, China); anhydrous ethanol and ammonia solution (concentration 25–28%) are both analytical reagent grade, purchased from Tianjin Tianli Chemical Reagents Co., Ltd. (Tianjin, China); quicklime, industrial grade, Tianjin Hongyan Reagent Factory (Tianjin, China); wheat flour, commercially available; boiled tung oil, industrial grade, Nanshan Tung Oil Factory in Gushixian County (Shenzhen, China); lithopone, industrial grade, Ganting Mining Co., Ltd. (Ganting, China); reference nano-zinc oxide (specifications 30 nm, 50 nm, and 90 nm), analytical reagent grade, Aladdin Reagents Co., Ltd. (Shanghai, China); water-based fluorocarbon coating, industrial grade, Dalian Zhenbang Fluorocarbon Coating Co., Ltd. (Dalian, China); acrylic pigment, industrial grade, Montmartre Office Supplies Store (Paris, France); all water used in the experiment is deionized water.

2.2. Preparation of Coating Materials

2.2.1. Preparation of Nano-Zinc Oxide

5 g of zinc nitrate hexahydrate and 3 g of anhydrous sodium carbonate were each dissolved in 30 mL of pure water, after which the zinc nitrate solution was transferred to a mechanically stirred 100 mL three-necked flask. Rapid injection of the sodium carbonate solution during vigorous room-temperature agitation through an auxiliary neck induced

immediate viscous sol formation, with continued stirring for an additional 5 min. The product was centrifuged at 4000 r/min for 10 min, the supernatant discarded, and the gel scraped into a beaker. The gel was resuspended in 60 mL of pure water, subjected to ultrasonication, and centrifuged again with supernatant removal; this water washing procedure was repeated twice using a total of 180 mL of distilled water. Subsequently, centrifugal washing with 1% (v/v) dilute ammonia solution was performed three times, utilizing 60 mL per wash, each cycle consisting of ultrasonication, centrifugation, and supernatant discard. Finally, washing with 60 mL anhydrous ethanol per cycle was conducted three times following the same ultrasonication-centrifugation sequence. The resulting gel was dried under vacuum at 40 °C for 12 h and then finely ground to yield the zinc oxide precursor, zinc carbonate.

The powder was taken (0.5 g) and calcined for 1 h at 450 °C in a tubular furnace to obtain the nano-zinc oxide powder [7,15,16].

2.2.2. Preparation of Base Layer Material

50 g of quicklime was added to 1000 g of distilled water and vigorously stirred. Following dissolution, the mixture was filtered to remove insoluble residues, yielding lime water. To this lime water, 400 g of wheat flour was gradually incorporated in 50–100 g increments under continuous stirring until a thin paste formed; this paste was then fermented at room temperature for 3 to 5 h. Subsequently, 450 mL of boiled tung oil was introduced and stirred to achieve a homogeneous mixture. Finally, a total of 1200 g of lithopone was added incrementally in 100–200 g portions, with thorough stirring after each addition, resulting in the formation of the base coat material [8,17,18].

2.2.3. Preparation of Transparent UV Resistant Crack-Resistant Coating Material

A dispersion of nano-zinc oxide was prepared by ultrasonicating 0.1 g of nano-zinc oxide powder in 40 mL of pure water for 10 min, yielding a homogeneous dispersion with a concentration of 2.5 mg/mL. This nano-zinc oxide dispersion was then introduced into a measured quantity of a water-based fluorocarbon coating according to the specified ratio. The mixture was homogeneously blended and subsequently subjected to an additional 10-min ultrasonication treatment, resulting in the formation of the compound coating [1].

2.2.4. Plate Coating

(1) Coat the glass slide

The coating was applied to the slide by roller coating with different proportions of mixed coatings, and the transparent coating was attained after drying at room temperature. The transparency and ultraviolet resistance of the coating were tested by UV-visible spectrophotometer [1].

(2) Coat the painted wooden board

Solid wood panels (120 × 80 × 20 mm) were coated with base layer materials applied using a putty knife to achieve full coverage of surface irregularities and ensure uniform smoothness. Following drying at room temperature, the primed surfaces were sanded with 400-grit sandpaper until smooth. A 1:1 (v/v) acrylic paint mixture was prepared and applied to the base layer material, with subsequent drying at room temperature. To facilitate direct UV resistance comparison, each panel was divided along its central axis by a pencil line. The prepared protective coating was then applied exclusively to the right section of this demarcation and dried under ambient conditions [2] (see Figure 1).

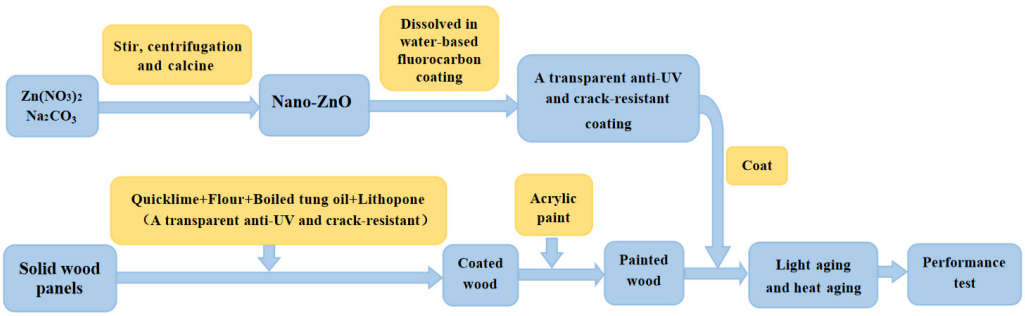

Figure 1. Diagram of technological process.

2.3. Testing

The appearance and particle size of nano-zinc oxide were tested using an H-7650 transmission electron microscope (Hitachi, Suzhou, China) and a Zetasizer Nano3600 laser particle size analyzer (Malvern, Shanghai, China). The UV shielding ability of nano-zinc oxide and composite coatings was tested using a UV-1800 UV-visible spectrophotometer (Shimadzu, Suzhou, China). The thermal properties of the coating were determined using the TGA (Thermal Gravimetric Analyzer) and DSC (Differential Scanning Calorimeter) methods from TA Instruments in the United States. The temperature range for thermal analysis was 20 to 800 °C, with a heating rate of 10 °C/min; the scanning calorimetry range was 20 to 350 °C, also at a heating rate of 10 °C/min, with an injection volume of approximately 2 mg. The coating was subjected to accelerated aging tests using a UV climate chamber (Suzhou Zhihe Environmental Test Equipment Co., Ltd., Suzhou, China). The chamber's program for each 24-h cycle includes 16 h of UV light exposure followed by 8 h of water spray, maintaining the chamber in a 50 °C water vapor environment. The test chamber uses four UV lamps, with each lamp positioned about 5 cm from the sample board, and the average UV intensity within the chamber is between 40,000 and 42,000 mw/m^2. A CS-10 color difference meter (CaiPu Technology Co., Ltd., Taizhou, China) was used to compare the color change in painted wooden boards after applying the protective coating [14,19–21].

3. Results and Discussion

3.1. Characterization of Homemade Nano-Zinc Oxide

3.1.1. Transmission Electron Microscopy Analysis

As can be seen from Figure 2, the original particle size of homemade nano-zinc oxide is about 20~30 nm, and the shape is mostly ellipsoidal to rod-shaped, with relatively uniform particle size.

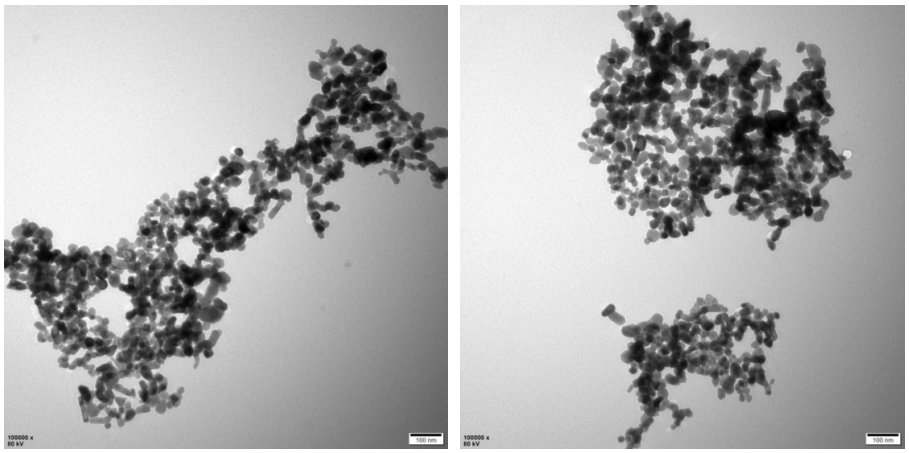

Figure 2. TEM images of self-made nano-zinc oxide (100,000×).

3.1.2. Ultraviolet-Visible Spectrophotometric Analysis

Select homemade nano-zinc oxide and three types of externally purchased nano-zinc oxides with specifications of 30 nm, 50 nm, and 90 nm, respectively, to ultrasonically prepare nano-dispersions at a concentration of 0.125 mg/mL. Using pure water as the reference, UV-visible spectrophotometry was employed to measure the UV and visible light transmittance of these powders. As shown in Figure 3, the maximum light transmittance of the homemade zinc oxide sample in the visible light region can reach over 92%, while the transmittance in the UV region from 200 to 400 nm is almost zero, indicating that its dispersion has both transparency and strong UV absorption capabilities; in contrast, the maximum light transmittance of the externally purchased nano-zinc oxide samples 1# and 2# at the same concentration is only around 73% in the visible light region, and the highest transmittance of the externally purchased nano-zinc oxide sample 3# in the visible light region is only about 60%. Additionally, it can be observed that the transmittance of the externally purchased samples in the UV region ranges from 1% to 10%, significantly lower than that of the homemade samples. Therefore, the externally purchased nano-zinc oxide samples are notably weaker than the homemade samples in terms of transparency and UV absorption capabilities [7,12,13].

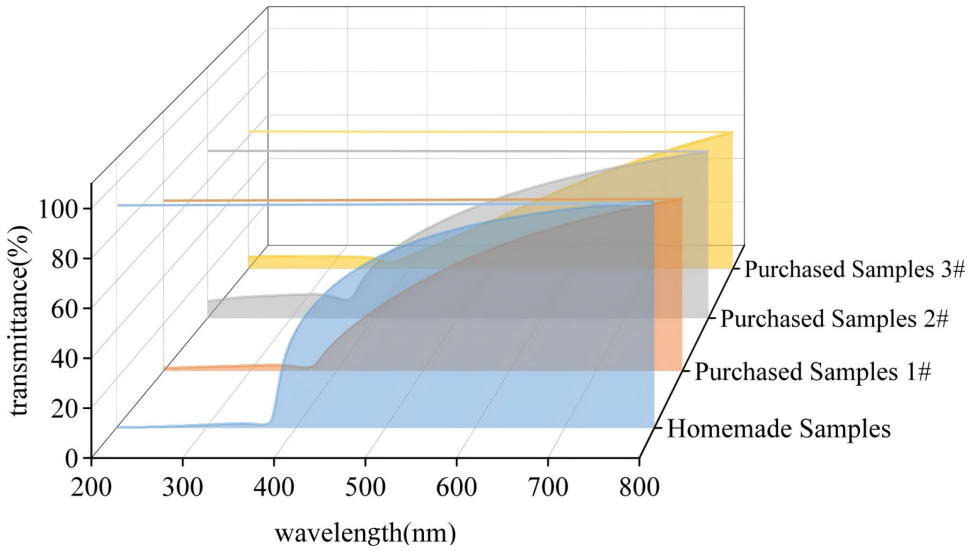

Figure 3. Compared curves of UV and visible light transmittance of homemade and purchased nano-zinc oxide.

3.1.3. Anti-Settling Test

Nanoparticles can exhibit unique properties not found in bulk materials across various fields because they maintain a uniform nanoscale dispersion for extended periods. This allows them to fully demonstrate characteristics such as small particle size, high specific surface area, high surface energy, and a large proportion of surface atoms [19]. If nanoparticles experience significant settling during use due to issues like excessive particle size or agglomeration, it will severely impact their performance [22].

For this purpose, based on the z-average and polydispersity index (PDI) of particle sizes measured using a laser particle size analyzer for various samples, sedimentation tests were conducted on self-prepared nano-zinc oxide and commercially available nano-zinc oxide ultrasonically dispersed in pure water at the same concentration. Specifically, several types of nanoparticles were ultrasonically dispersed in pure water of equal mass, and their sedimentation over time was observed and recorded [7,13]. The detailed results are shown in Table 1.

Table 1. Particle detection data and sedimentation time of nano-zinc oxide samples.

Name of Sample	Grain Size Z-Mean	PDI	Settling Time/ Complete Settling Time (h)
Homemade Samples	150 ± 20	0.18	120/576
Purchased Samples 1#	300 ± 50	0.28	3/24
Purchased Samples 2#	400 ± 50	0.36	1/11
Purchased Samples 3#	500 ± 20	0.45	0.5/6

As shown in Table 1, compared to the results from transmission electron microscopy, the particle size test values of several types of nano-zinc oxide, including the homemade sample, are all higher. The reasons for this discrepancy can be attributed to two points: First, the laser particle size analyzer measures the hydrated diameter of the sample. Nano-zinc oxide has strong hydrophilicity, and its surface is coated with water molecules, leading to larger measured particle sizes. Second, the particle size analyzer uses the principle of light scattering to measure the particle size. The z-average particle size is calculated by fitting the sample's particles into standard spheres and then statistically analyzing them. However, after calcination, the shape of the zinc oxide samples is not very regular, resulting in poor sphericity and thus introducing some error in the measurement. Despite these issues, the results from the particle size analyzer can still serve as a reference. It is evident that the z-average particle size and PDI of the homemade samples are lower than those of the purchased samples. The settling properties of the samples are also directly related to their particle size and polydispersity coefficient. The purchased Sample 3#, which has the largest particle size and polydispersity coefficient, showed significant settling within 0.5 h and complete settling within 6 h. The purchased Samples 2# and 1# have slightly better anti-settling capabilities compared to Sample 3#, but they also exhibit noticeable settling within 1 to 3 h, with complete settling occurring after 11 h and 24 h. In contrast, the homemade samples did not show significant settling within the observed 12 h. Further observation revealed that the complete settling time of the self-made samples was as long as 24 days (576 h). This clearly demonstrates a significant difference in anti-settling capability between the purchased nano-zinc oxide and the homemade nano-zinc oxide. Therefore, in subsequent experiments, the homemade zinc oxide was used as the UV-resistant component in the coating [7,13,14].

3.2. Performance Test of Transparent Uv Resistant Crack-Resistant Coating

3.2.1. Transparency and Ultraviolet Absorption Capacity

To quickly obtain the transparency and UV resistance data of the compounded coating material, different nano-zinc oxide content coatings were roll-coated on transparent slides. After drying at room temperature, a series of transparent, UV-resistant composite coatings were prepared. Using a blank slide as the reference, the UV shielding ability of the coatings was tested with a UV-visible spectrophotometer. The test results are shown in Figure 4 [7,13].

As shown in Figure 4, as the addition ratio of nano-zinc oxide increases from 0.1% to 0.5%, the maximum transmittance of the coating in the visible light region (400–800 nm) decreases from 88% to 65%. In the ultraviolet region, except for the coating with 0.1% nano-zinc oxide content, which has the highest UV transmittance at 8%, all other coatings have a UV transmittance of less than 2%. The maximum transmittance in the visible light region for coatings with 0.2% and 0.3% nano-zinc oxide content is both greater than 80%, and the UV transmittance is less than 1%. However, at 0.5% nano-zinc oxide content, although the UV transmittance is almost zero, the transmittance in the visible light region drops significantly, indicating that the concentration of nanoparticles is sufficient to affect the

transparency of the coating. This suggests that the concentration of nanoparticles in the coating is too high, leading to some degree of agglomeration between particles and an increase in macroscopic particle size. Therefore, it is not true that more nanoparticles are always better; the key is to ensure that each nanoparticle can effectively scatter UV light. Considering all factors, subsequent experiments will use a 0.2% addition ratio of nano-zinc oxide [7,13,14,23].

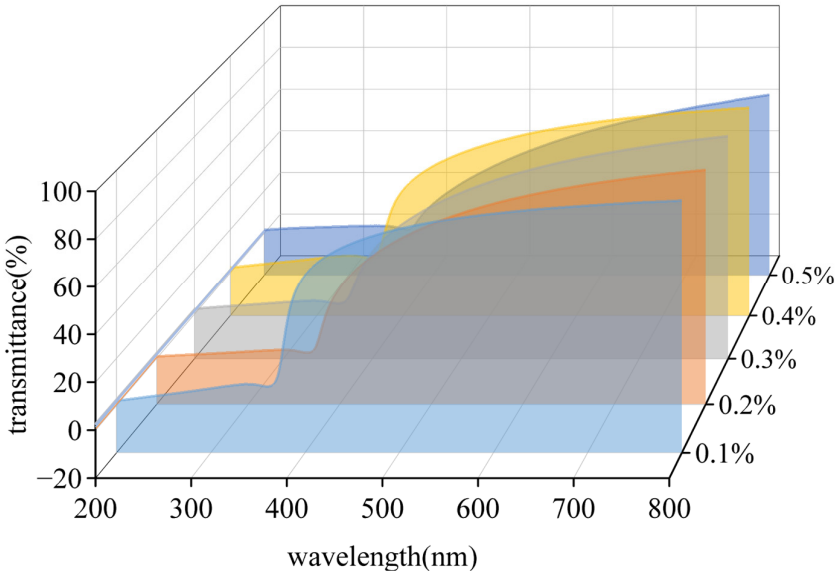

Figure 4. Compared curves of UV and visible light transmittance of composite coatings with different nano-zinc oxide content.

3.2.2. Thermal Performance Analysis of Coating Materials

In order to understand the thermal decomposition properties and thermodynamic parameters such as glass transition temperature (Tg) of composite coating materials, the coating materials were analyzed by thermogravimetric analyzer (TG) and differential scanning calorimeter (DSC).

(1) Thermogravimetric (TG) analysis

As shown in Figure 5, the thermal decomposition temperature range of the composite coating material is between 300 °C and 500 °C, with a total weight loss rate of 85.34%. The remaining weight should be the residual carbon from the components of water-based fluorocarbon coating decomposed under a nitrogen atmosphere, along with a small amount of inorganic nano-zinc oxide. From the details of the weight loss curve, the material is very stable before 100 °C, with virtually no weight loss; between 100 °C and 300 °C, the weight loss rate is approximately 10.70%, which is likely due to the decomposition of small molecules such as additives in the water-based fluorocarbon coating. Within the temperature range of 300 °C to 400 °C, the material decomposes rapidly, and at 500 °C, it has almost completely decomposed, indicating that the main component of the selected water-based fluorocarbon coating exhibits good thermal stability before 300 °C.

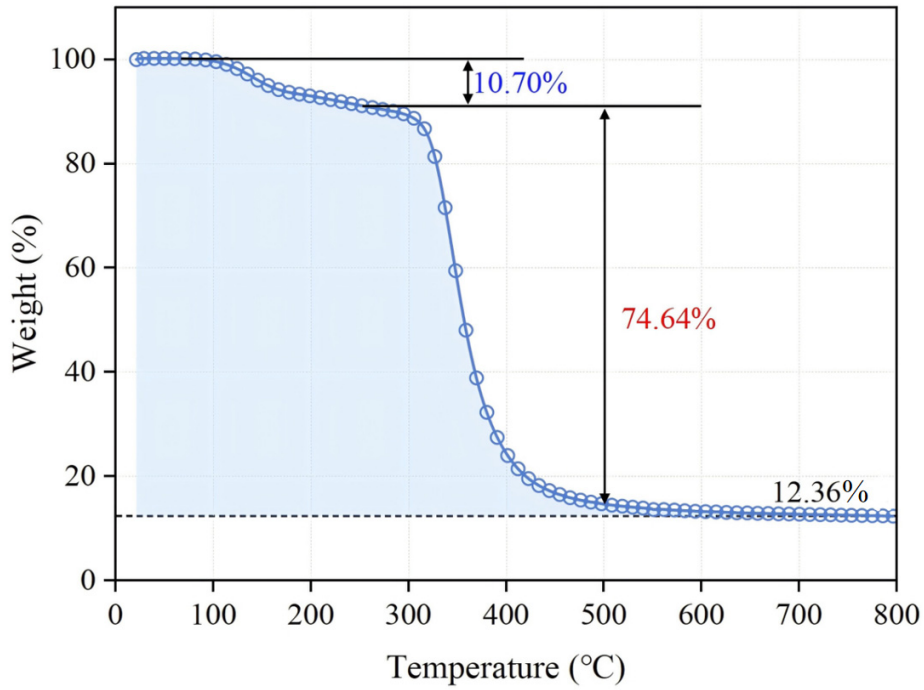

Figure 5. TG curve of composite coating.

(2) Differential scanning calorimetry (DSC) analysis

As shown in Figure 6, the glass transition temperature (Tg) of the composite material is at 268.71 °C, indicating that the material maintains its rigidity and basic molecular structure up to this temperature. Beyond this point, the molecular chain mobility increases, leading to a decrease in coating stability. Combining the results from thermogravimetric analysis, it can be concluded that the material remains stable both thermodynamically and structurally until 250 °C.

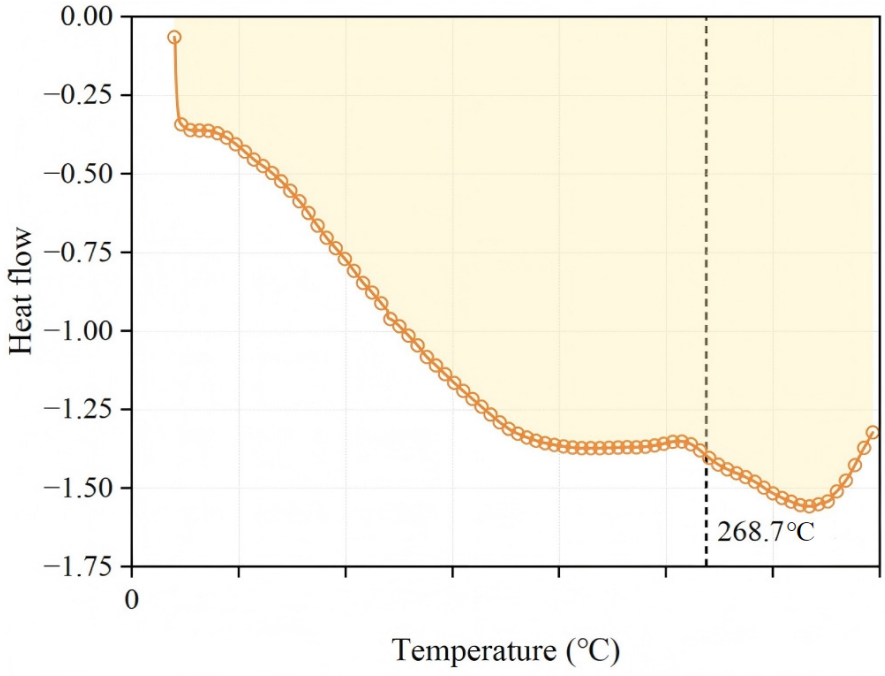

Figure 6. DSC analysis result of composite coating.

3.2.3. Ultraviolet Accelerated Aging Test of Painted Protective Coating

A three-color painted wood board coated with red, green, and blue acrylic pigments was selected, and a transparent anti-UV crack-resistant coating material was applied to the right half of the wood board. The samples were placed in the UV weathering test chamber for accelerated aging for 20 d [7,14,24]. The surface state of each sample after aging is shown in Figure 7.

As shown in Figure 7, the left half of the samples without protective coating material showed obvious cracking and fading, while the right half with the protective coating remained bright and intact. Among them, the red sample had the most severe cracking on its unprotected side, followed by the green sample, with the blue sample showing slightly less damage.

The color difference values of the red, green, and blue sample panels before and after accelerated aging were tested using a colorimeter (Figure 8). As shown in the figure, the degree of color degradation varies among different color samples after accelerated aging. Generally, the color difference values of unpainted protective coating layers are significantly higher than those of painted protective coating layers. This indicates that the transparent, UV-resistant, and crack-resistant coating material has a significant protective effect on the painted layer under conditions such as UV light, water–spray and water–vapor fumigation. By comparing the color difference values of each color sample after exposure to UV light, it can be observed that the red pigment has the highest color difference value, indicating its greater sensitivity to UV light. In contrast, the sensitivity of green and blue pigments to UV light is significantly lower than that of the red pigment [25–27].

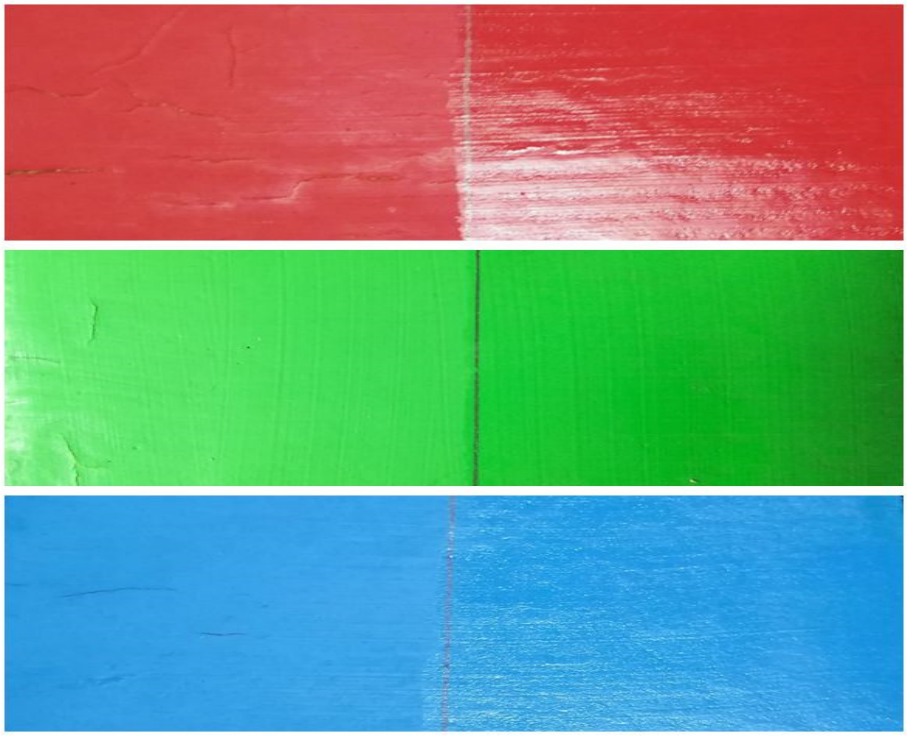

Figure 7. Photographs of red, green, and blue painted wood plates after 20 days accelerated aging in UV weathering chamber.

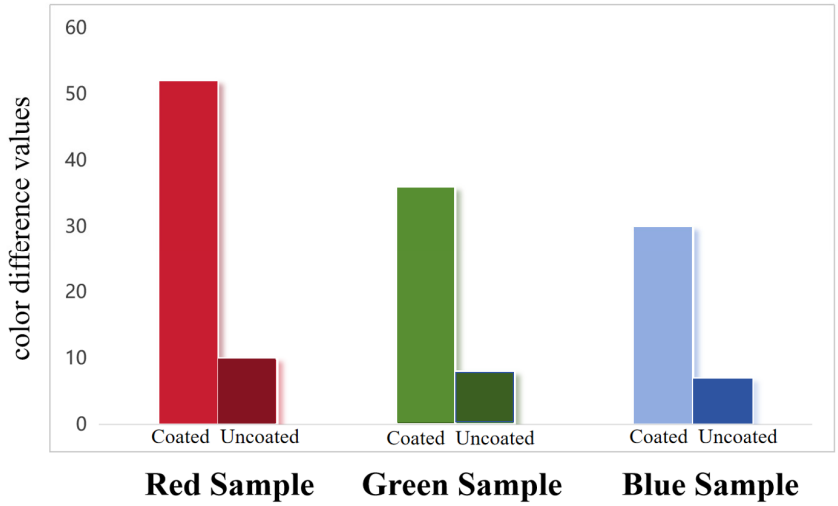

Figure 8. Contrast diagram of color difference in red, green, and blue painted wood plate (coated: The outer surface of sample panels were coated with transparent water-based fluorocarbon coating. Uncoated: there were not transparent water-based fluorocarbon coating on the outer surface of sample panels).

3.3. Conservation Experiment of Paintings in Changwu Zhaoren Temple and Xianyang Confucian Temple

A weather-resistant nano-coating material was prepared by using self-made nano-zinc oxide as the UV absorber and water-based fluorocarbon coating as the binder. Taking slides and painted wooden boards as the coating objects, respectively, the transparency, ultraviolet absorption capacity, and weather resistance of the coating were detected by ultraviolet-visible spectrophotometer and ultraviolet light weather resistance test chamber. The test results show that the coating material not only has high transparency but also has obvious color retention and crack resistance effects on the painted layer. At present, this coating material has been successfully applied in the experimental research on the protection of painted cultural relics in Xianyang Museum and Zhaoren Temple in Changwu.

There are a large number of precious ancient architectural paintings on these ancient buildings. Over time, due to the periodic changes in light, temperature, and humidity, oxidation, erosion by harmful gases and pollution from various dust sources, the paintings and the paints on the columns have developed diseases such as blurring and fading of colors and patterns, as well as lifting and peeling of the painting layers, causing them to lose their original appearance. Some have even vanished completely and become unrecognizable. It affects tourists' visits and scientific research. In order to test the effect of protective materials in protecting painted paintings in a real environment, a corner of the painted layer on the north side of a corridor pillar of Changwu Zhaoren Temple and a side room of Xianyang Confucian Temple (not a site area) were selected as the test areas for on-site protection comparison tests, as shown in Figure 9. Subsequently, the intensities of outdoor ultraviolet light in the Xianyang area were collected. The illuminance monitored by the outdoor meteorological station of Xianyang from March to August 2023 ranged from 5075.89 to 124,913.88 lx, and the ultraviolet intensity ranged from 0.24 to 1835.33 $\mu w/cm^2$. From March to August 2023, the atmospheric temperature and humidity monitored by the outdoor meteorological station in Xianyang ranged from 4.1 °C to 39.7 °C, with a fluctuation range of 35.6 °C and an average temperature of 23.6 °C. The humidity ranged from 9.7% to 89.7%, with a fluctuation range of 80.0%, and the average humidity was 51.5%. After continuous observations for 120 days and 360 days, the protective effect of the painted layer was good (Figure 9).

Apply protective coating
(north side corridor of Zhaoren Temple)

Painting protective coating (one corner of the painted layer in the side room of Xianyang Wenmiao)

After protection (120 days)

After protection (120 days)

After protection (360 days)

After protection (360 days)

Figure 9. Photos of the experimental process of painting protective coating in Zhaoren Temple and Xianyang Confucian Temple (the area enclosed by the white frame in the image is the experimental zone).

4. Conclusions

In this study, a transparent, weather-resistant coating was prepared by compounding self-made nano-zinc oxide with a water-based fluorocarbon coating. Both laboratory and field tests have shown that this coating can significantly resist UV rays delay fading and cracking while preserving the original appearance of the painted paintings. It is easy to apply and has been used for the protection of painted paintings in the Confucian Temple of Xianyang and the Zhaoren Temple of Changwu. It has solved the problem of fading and cracking of ancient architectural paintings due to environmental aging and provided a reference for the long-term protection of ancient architectural paintings.

Author Contributions: The manuscript was prepared through contributions of all authors. J.Y. planned the study together with J.C. and wrote most of the manuscript; J.Z., T.W. and X.Y. conducted all data analysis, and H.Y., W.Z. and S.H. designed part of the experiment. All authors have read and agreed to the published version of the manuscript.

Funding: This work was supported by the National Natural Science Foundation of China (No. 22102094), State Administration of Cultural Heritage Science and Technology Research Project (No. 2023ZCK028), and the Fundamental Research Funds for the Central Universities (No. GK 202205024, GK202309016), the Key Laboratory of Archeological Exploration and Cultural Heritage Conservation Technology (Northwestern Polytechnical University), Ministry of Education (Project No. 2024KFT01).

Institutional Review Board Statement: Not applicable.

Informed Consent Statement: Not applicable.

Data Availability Statement: The original contributions presented in the study are included in the article, further inquiries can be directed to the corresponding author.

Acknowledgments: The authors would like to thank the Engineering Research Center of Historical and Cultural Heritage Protection, Ministry of Education, Shaanxi Normal University for their support and research cooperation.

Conflicts of Interest: The authors declare no competing interests.

References

1. Liu, D.; Cao, K.; Tang, Y.; Zhang, J.; Meng, X.; Ao, T.; Zhang, H. Study on Weathering Corrosion Characteristics of Red Sandstone of Ancient Buildings Under the Perspective of Non-Destructive Testing. *J. Build. Eng.* **2024**, *85*, 108520. [CrossRef]
2. Yang, X.; Li, C.; Wang, L.; Yang, C.; Zhang, S.; Gao, J.; Qiu, J. The Characteristics of Ancient Residence Wood from the Qing Dynasty in Yunnan Province. *Coatings* **2024**, *14*, 200. [CrossRef]
3. Qian, C.; Li, M.; Liao, H.; Zhang, C.; Li, H. Research on the Vibration Fatigue Characteristics of Ancient Building Wood Materials. *Buildings* **2024**, *14*, 2840. [CrossRef]
4. Hang, T.T.X.; Dung, N.T.; Truc, T.A.; Duong, N.T.; Van Truoc, B.; Vu, P.G.; Hoang, T.; Thanh, D.T.M.; Olivier, M.-G. Effect of silane modified nano ZnO on UV degradation of polyurethane coatings. *Prog. Org. Coat.* **2015**, *79*, 68–74. [CrossRef]
5. Nguyen-Tri, P.; Tran, H.N.; Plamondon, C.O.; Tuduri, L.; Vo, D.-V.N.; Nanda, S.; Mishra, A.; Chao, H.-P.; Bajpai, A. Recent progress in the preparation, properties and applications of superhydrophobic nano-based coatings and surfaces: A review. *Prog. Org. Coat.* **2019**, *132*, 235–256. [CrossRef]
6. Ghamarpoor, R.; Fallah, A.; Jamshidi, M. Investigating the use of titanium dioxide (TiO_2) nanoparticles on the amount of protection against UV irradiation. *Sci. Rep.* **2023**, *13*, 9793. [CrossRef]
7. Yang, H.; Han, K.; Fu, P.; Zhao, P.; Li, Y. Evaluation of the Reinforcement Performance of Protective Materials for Commonly Used Pigment Layers in Ancient Architectural Color Paintings. *Sci. Conserv. Archaeol.* **2024**, *36*, 94–106.
8. Knežević, N.Ž.; Ilić, N.; Djokic, V.; Petrović, R.; Janaćković, D. Mesoporous Silica and Organosilica Nanomaterials as UV-Blocking Agents. *ACS Appl. Mater. Interfaces* **2018**, *10*, 20231–20236. [CrossRef]
9. A Carboxylated Modified Nano-Titanium Dioxide UV Shielding Agent and Its Preparation Method. X Technology. 2021. Available online: https://www.xjishu.com/zhuanli/25/202110797499.html (accessed on 23 September 2025).
10. Zhou, J.; Tan, Z.; Liu, Z.; Jing, M.; Liu, W.; Fu, W. Preparation of transparent fluorocarbon/TiO_2-SiO_2 composite coating with improved self-cleaning performance and anti-aging property. *Appl. Surf. Sci.* **2017**, *396*, 161–168. [CrossRef]

11. Materials Characterization. Available online: https://www.sciencedirect.com/journal/materials-characterization (accessed on 23 September 2025).
12. Liu, H. *Research on the Functionalization of Nano-Zinc Oxide and the Preparation and Properties of Its UV—Shielding Composites*; South China University of Technology: Guangzhou, China, 2022.
13. Li, D.; Yang, C.; Li, P.; Yu, L.; Zhao, S.; Li, L.; Kang, H.; Yang, F.; Fang, Q. Synthesis and Properties of the Novel High—Performance Hydroxyl—Terminated Liquid Fluoroelastomer. *Polymers* **2023**, *15*, 2574. [CrossRef]
14. Fan, T.; Feng, X.; Yang, J. Protection Practice and Reflection of Ancient Architectural Color Paintings in Jiangsu. *Sci. Res. Chin. Cult. Relics* **2022**, *4*, 29–40.
15. Wadhwa, P.; Sharma, S.; Sahu, S.; Sharma, A.; Kumar, D. A review of nanoparticles characterization techniques. *Curr. Nano-mater.* **2022**, *5*, 7. [CrossRef]
16. Doni, M.; Fierascu, I.; Fierascu, R.C. Recent Developments in Materials Science for the Conservation and Restoration of Historic Artifacts. *Appl. Sci.* **2024**, *14*, 11363. [CrossRef]
17. Elkady, F.M.; Badr, B.M.; Saied, E.; Hashem, A.H.; Abdulrahman, M.S.; Alkherkhisy, M.M.; Selim, T.A.; Alshabrmi, F.M.; Alatawi, E.A.; Alkhayl, F.F.A.; et al. Mycosynthesis of zinc oxide nanoparticles using Mucor racemosus with their antimicrobial, antibiofilm, anticancer and antioxidant activities. *Sci. Rep.* **2025**, *15*, 1–22. [CrossRef]
18. Guo, X.; Guo, R.; Fang, M.; Wang, N.; Liu, W.; Pei, H.; Liu, N.; Mo, Z. A novel composite protective coating with UV and corrosion resistance: Load floating and self-cleaning performance. *Ceram. Int.* **2022**, *48*, 17308–17318. [CrossRef]
19. Reinosa, J.J.; Docio, C.M.Á.; Ramírez, V.Z.; Lozano, J.F.F. Hierarchical nano ZnO-micro TiO_2 composites: High UV protection yield lowering photodegradation in sunscreens. *Ceram. Int.* **2018**, *44*, 2827–2834. [CrossRef]
20. Shnoudeh, A.J.; Hamad, I.; Abdo, R.W.; Qadumii, L.; Jaber, A.Y.; Surchi, H.S.; Alkelanyet, S.Z. Chapter 15—Synthesis, Characterization, and Applications of Metal Nanoparticles. In *Biomaterials and Bionanotechnology*; Tekade, R.K., Ed.; ScienceDirect. Academic Press: Cambridge, MA, USA, 2019; pp. 527–612.
21. Fu, P.; Teri, G.-L.; Chao, X.-L.; Li, J.; Li, Y.-H.; Yang, H. Modified Graphene-FEVE Composite Coatings: Application in the Repair of Ancient Architectural Color Paintings. *Coatings* **2020**, *10*, 1162. [CrossRef]
22. Al-Fadhily, Z.M.; Abdul-Hadi, M. A Novel Coating of Orthodontic Archwires with Chlorhexidine Hexametaphosphate Nanoparticles. *Int. J. Biomater.* **2023**, *2023*, 9981603. [CrossRef]
23. Fistos, T.; Fierascu, I.; Doni, M.; Chican, I.E.; Fierascu, R.C. A Short Overview of Recent Developments in the Application of Polymeric Materials for the Conservation of Stone Cultural Heritage Elements. *Materials* **2022**, *15*, 6294. [CrossRef]
24. Han, K.; Liu, J.; Hao, F.; Wang, J.; Yuan, J.; Pan, Z.; Pan, M. An adaptive waterborne fluorocarbon coatings with Anti-Flashing Rust, Antibiofouling, and Self-Repairing properties. *Chem. Eng. J.* **2024**, *495*, 153644. [CrossRef]
25. Pino, F.; Fermo, P.; La Russa, M.; Ruffolo, S.; Comite, V.; Baghdachi, J.; Pecchioni, E.; Fratini, F.; Cappelletti, G. Advanced mortar coatings for cultural heritage protection. Durability towards prolonged UV and outdoor exposure. *Sci. Pollut. Res.* **2017**, *24*, 12608–12617. [CrossRef] [PubMed]
26. Oancea, A.V.; Bodi, G.; Cernescu, A.; Spiridon, I.; Nicolescu, A.; Drobota, M.; Cotofana, C.; Simionescu, B.C.; Olaru, M. Protective coatings for ceramic artefacts exposed to UV ageing. *NPJ Mater. Degrad.* **2023**, *7*, 1–13. [CrossRef]
27. Cinteză, L.O.; Tănase, M.A. Multifunctional ZnO Nanoparticle: Based Coatings for Cultural Heritage Preventive Conservation. In *Thin Films*; IntechOpen eBooks: London, UK, 2021.